


230 s room-temperature storage time and 1.14 eV hole localization energy in $\text{In}_{0.5}\text{Ga}_{0.5}\text{As}$ quantum dots on a GaAs interlayer in GaP with an AIP barrier

Cite as: Appl. Phys. Lett. **106**, 042102 (2015); <https://doi.org/10.1063/1.4906994>

Submitted: 17 November 2014 . Accepted: 08 January 2015 . Published Online: 28 January 2015

Leo Bonato , Elisa M. Sala, Gernot Stracke, Tobias Nowozin, André Strittmatter, Mohammed Nasser Ajour, Khaled Daqrouq, and Dieter Bimberg



View Online



Export Citation



CrossMark

ARTICLES YOU MAY BE INTERESTED IN

[Growth and structure of \$\text{In}_{0.5}\text{Ga}_{0.5}\text{Sb}\$ quantum dots on GaP\(001\)](#)

Applied Physics Letters **109**, 102102 (2016); <https://doi.org/10.1063/1.4962273>

[Indirect and direct optical transitions in \$\text{In}_{0.5}\text{Ga}_{0.5}\text{As}/\text{GaP}\$ quantum dots](#)

Applied Physics Letters **104**, 123107 (2014); <https://doi.org/10.1063/1.4870087>

[Hole-based memory operation in an \$\text{InAs}/\text{GaAs}\$ quantum dot heterostructure](#)

Applied Physics Letters **95**, 242114 (2009); <https://doi.org/10.1063/1.3275758>

Lock-in Amplifiers
up to 600 MHz



Watch



AIP
Publishing

230 s room-temperature storage time and 1.14 eV hole localization energy in $\text{In}_{0.5}\text{Ga}_{0.5}\text{As}$ quantum dots on a GaAs interlayer in GaP with an AIP barrier

Leo Bonato,^{1,a)} Elisa M. Sala,¹ Gernot Stracke,¹ Tobias Nowozin,¹ André Strittmatter,¹ Mohammed Nasser Ajour,² Khaled Daqrouq,² and Dieter Bimberg^{1,2}

¹Institut für Festkörperphysik, Technische Universität Berlin, Hardenbergstr. 36, 10623 Berlin, Germany

²King Abdulaziz University, Jeddah, Saudi Arabia

(Received 17 November 2014; accepted 8 January 2015; published online 28 January 2015)

A GaP n^+p -diode containing $\text{In}_{0.5}\text{Ga}_{0.5}\text{As}$ quantum dots (QDs) and an AIP barrier is characterized electrically, together with two reference samples: a simple n^+p -diode and an n^+p -diode with AIP barrier. Localization energy, capture cross-section, and storage time for holes in the QDs are determined using deep-level transient spectroscopy. The localization energy is $1.14(\pm 0.04)$ eV, yielding a storage time at room temperature of $230(\pm 60)$ s, which marks an improvement of 2 orders of magnitude compared to the former record value in QDs. Alternative material systems are proposed for still higher localization energies and longer storage times. © 2015 AIP Publishing LLC.

[<http://dx.doi.org/10.1063/1.4906994>]

At present, solid-state memory technology is fundamentally divided into volatile memories (e.g., DRAM) and non-volatile memories (e.g., Flash). Overcoming this divide by developing fast-access non-volatile memory “would initiate a revolution in computer architecture.”¹ The trade-off between storage time and data access time can be overcome using quantum dots (QDs).² The potential of QDs as storage elements in memory devices was demonstrated before.^{3,4} The longest storage of charge carriers in QDs hitherto measured at room temperature is 1.6 s for holes in InAs/GaAs QDs with an $\text{Al}_{0.9}\text{Ga}_{0.1}\text{As}$ barrier² and the highest measured localization energy is $E_{loc} = 0.8$ eV for GaSb QDs in GaAs with an $\text{Al}_{0.3}\text{Ga}_{0.7}\text{As}$ barrier.⁵ 8-band $\mathbf{k} \cdot \mathbf{p}$ calculations show that storage times longer than 10 years can be obtained by using heterostructures with much larger E_{loc} .⁶ In particular, a hole localization energy of about 0.6 eV is expected for $\text{In}_{0.5}\text{Ga}_{0.5}\text{As}$ QDs in GaP.⁷ An AIP barrier would provide an additional 0.5 eV, yielding a total emission barrier between 1.0 eV and 1.1 eV for holes trapped in the QDs.⁸

The key to successfully growing InGaAs QDs in GaP using metal-organic chemical vapor deposition (MOCVD) is a GaAs interlayer.^{9,10} Such QDs with a nominal In content of 25% yield a mean activation energy of 490 meV.⁹ QDs with an increased In content (50%) were grown and characterized with atomic force microscopy (AFM), cross-sectional scanning tunneling microscopy (X-STM), and photoluminescence spectroscopy (PL).¹¹ However, a measurement of the electronic properties, such as their capture cross-section and activation energy, is still missing.

In this letter, we report on the electronic properties of a set of three samples, the main one containing $\text{In}_{0.5}\text{Ga}_{0.5}\text{As}$ QDs grown on a GaAs interlayer in a GaP matrix, with an additional AIP barrier aimed at increasing the localization energy of holes in the QDs, and thus the storage time. The electronic properties of the QDs are investigated using deep level transient spectroscopy (DLTS)¹² in order to determine activation energy and capture cross-section. The storage

time at room temperature is extrapolated from these parameters.

Since the electric fields at which the measurements are performed are comparatively small and the temperatures of interest high, tunneling emission from QDs can be neglected¹³ and the dominating process is thermal emission.¹⁴ The thermal emission rate of holes from QDs can be expressed as¹⁵

$$e_a = \gamma T^2 \sigma_\infty \exp\left(-\frac{E_a}{k_B T}\right), \quad (1)$$

where E_a is the activation energy, k_B the Boltzmann constant, T the temperature, σ_∞ the apparent capture cross section for $T = \infty$, and γ a temperature-independent constant. The storage time is the inverse of the thermal emission rate ($\tau = 1/e_a$) and therefore depends solely on the energy barrier (activation energy) E_a , which the holes have to overcome during the emission process, and on the apparent capture cross section σ_∞ . The cross section measures the probability of scattering free holes from the surrounding matrix into the QD. It is worth pointing out that in our case E_a will consist of the sum of the localization energy of the QD ensemble and the height of the AIP barrier.

The basic structure of the three measured samples (which is depicted in the inset of Fig. 1) is a GaP n^+p -diode (sample A), which is used as reference sample. In sample B, a layer of 20 nm AIP is embedded in the p -doped segment of the junction. The lowly p -doped segment of Sample C includes a 20 nm thick AIP layer (which acts as an emission barrier for charge-carriers in the QDs) and a layer of $\text{In}_{0.5}\text{Ga}_{0.5}\text{As}$ QDs separated from the AIP barrier by 2 nm of intrinsic GaP. The QD layer is composed of 0.8 monolayers (ML) of $\text{In}_{0.5}\text{Ga}_{0.5}\text{As}$ deposited on 2 ML of GaAs. The purpose of the GaAs interlayer is to enable the controlled formation of the $\text{In}_{0.5}\text{Ga}_{0.5}\text{As}$ QDs via the Stranki-Krastanow (SK) growth mode.⁹

All samples were grown on p -doped GaP (001) substrates using MOCVD. The 500 nm thick p^+ -doped

^{a)}Electronic mail: leo.bonato@tu-berlin.de

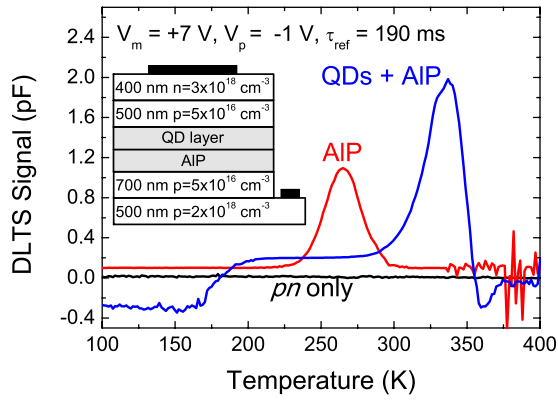


FIG. 1. Comparison of conventional DLTS measurements on the different samples (offset for reading ease). Inset: Sketch of sample structure.

($p = 2 \times 10^{18} \text{ cm}^{-3}$) GaP contact layer and the 700 nm lowly p -doped ($p = 5 \times 10^{16} \text{ cm}^{-3}$) GaP layer were grown at 750°C . The 20 nm AIP barrier and 2 nm GaP were grown at 800°C . For the QD layer, the growth temperature was lowered to 500°C . The purpose of the 2 nm of GaP is to protect the AIP surface from adsorbing impurities while cooling down to the QD growth temperature. Details about the QD growth can be found in Ref. 11. After a growth interruption of 200 s, the QDs were capped with 6 nm of intrinsic GaP. Subsequent layers were grown at 620°C . Zn (for p) and Si (for n) were used as dopants.

The processing involves standard optical lithography and dry etching techniques, yielding round mesa structures of $200 \mu\text{m}$ and $400 \mu\text{m}$ radius. The contacts are evaporated thermally and annealed at 400°C for 3 min, where Ni/AuGe/Ge is used for the n -side and Ni/Zn/Au for the p -side.^{16–18}

The samples are characterized with both conventional¹² and charge-selective DLTS.^{6,19} The bias voltage range in which charging and discharging of the QDs occur is determined first by means of capacitance–voltage (C – V) spectroscopy. In conventional DLTS, the reverse bias (V_m) is set such that the QDs are completely discharged at the beginning of the measurement. The DLTS cycle starts with a forward bias pulse (V_p) to charge the QDs. Then, the applied voltage returns to the measurement (reverse) bias and the capacitance transient due to the discharge of the QDs is observed. The emission times at different temperatures are obtained using the double box-car averaging technique and are then plotted in an Arrhenius plot to calculate E_a and σ_∞ . In the charge-selective DLTS mode, the write pulse is much smaller and chosen in such a way that only a few holes (ideally one hole per QD) enter and leave the QDs in each cycle. The DLTS cycle is then repeated with a different reverse bias, thus probing all internal levels of the QDs. The capacitance transients are measured at a frequency of 1 MHz and an AC voltage of 100 mV.

Sample A: For conventional DLTS, the measurement bias is set to $V_m = 7.0 \text{ V}$ (reverse) and the pulse to $V_p = -1.0 \text{ V}$ (forward). For charge-selective DLTS, the measurement bias ranges from $V_m = 7.0 \text{ V}$ to $V_m = 0.0 \text{ V}$ in steps of 1.0 V , while pulsing to $V_p = V_m - 1.0 \text{ V}$.

Sample B: Conventional: $V_m = 7.0 \text{ V}$, $V_p = -1.0 \text{ V}$. Charge-selective: $V_m = 7.0 \text{ V}$ to $V_m = 0.0 \text{ V}$ in steps of 1.0 V , $V_p = V_m - 1.0 \text{ V}$.

TABLE I. Mean, ensemble activation energies for samples B and C. Sample A does not show any peak.

Sample	E_a (eV)	σ_∞ (cm^2)
A	—	—
B	$0.47(\pm 0.07)$	$3.8(\pm 0.9) \times 10^{-17}$
C	$0.59(\pm 0.09)$	$2.1(\pm 0.5) \times 10^{-17}$

Sample C: Conventional: $V_m = 7.0 \text{ V}$, $V_p = -1.0 \text{ V}$. Charge-selective: $V_m = 6.5 \text{ V}$ to $V_m = 0.0 \text{ V}$ in steps of 0.5 V , $V_p = V_m - 0.5 \text{ V}$.

The temperature is swept from 100 K to 400 K in steps of 1.5 K. In all measurements, the charging pulse lasted 2 s and the discharge transient was recorded for 18 s. We chose the pulse width such that the charging process was always completed before the pulse ended.

All DLTS measurements were analysed using τ_{ref} ranging from 4 ms to 10.6 s. The conventional DLTS measurements are shown in Fig. 1 for all samples for a reference time $\tau_{\text{ref}} = 190 \text{ ms}$. As expected, the reference sample (A) shows no relevant features. Moreover, the peaks shown by samples B and C are clearly separated in temperature, indicating that they have a different origin. The mean, ensemble activation energies are listed in Table I, along with their error.

The charge-selective DLTS measurements on sample C are presented in Fig. 2. Fig. 3 compares the activation energies and capture cross sections extracted from the charge-selective DLTS measurements on samples B and C.

The peak in Fig. 2 remains at the same temperature for all voltages $V_m \leq 2.5 \text{ V}$. At that point, it starts shifting to higher temperatures, until it disappears completely for $V_m = 6.0 \text{ V}$ and $V_m = 6.5 \text{ V}$. Correspondingly, the measured activation energy (Fig. 3(a)) starts off at about $0.90(\pm 0.01) \text{ eV}$ and gradually increases until $1.40(\pm 0.07) \text{ eV}$ for $V_m = 5.5 \text{ V}$. The capture cross-section (Fig. 3(b)) follows a similar pattern, starting off at about $4(\pm 1) \times 10^{-13} \text{ cm}^2$ and increasing until $4(\pm 6) \times 10^{-6} \text{ cm}^2$. Since the peak for $V_m = 5.5 \text{ V}$ is very small, the accuracy of the estimate of the corresponding activation energy is also small. Furthermore, the activation energies for $V_m = 5.0 \text{ V}$ and $V_m = 4.5 \text{ V}$ appear to be very close to

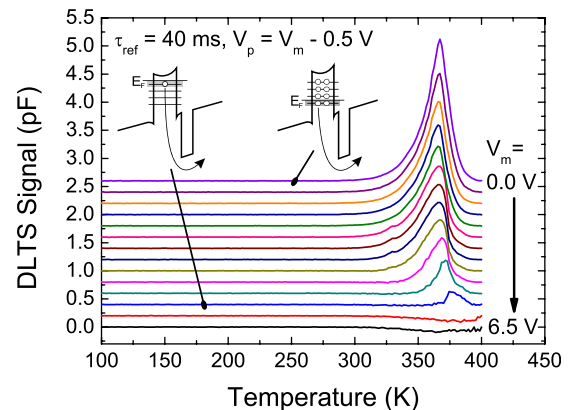


FIG. 2. Charge-selective DLTS measurements on sample C for reference time $\tau_{\text{ref}} = 40 \text{ ms}$. The schematic emission process from the QDs is sketched and pointed to the corresponding signal.

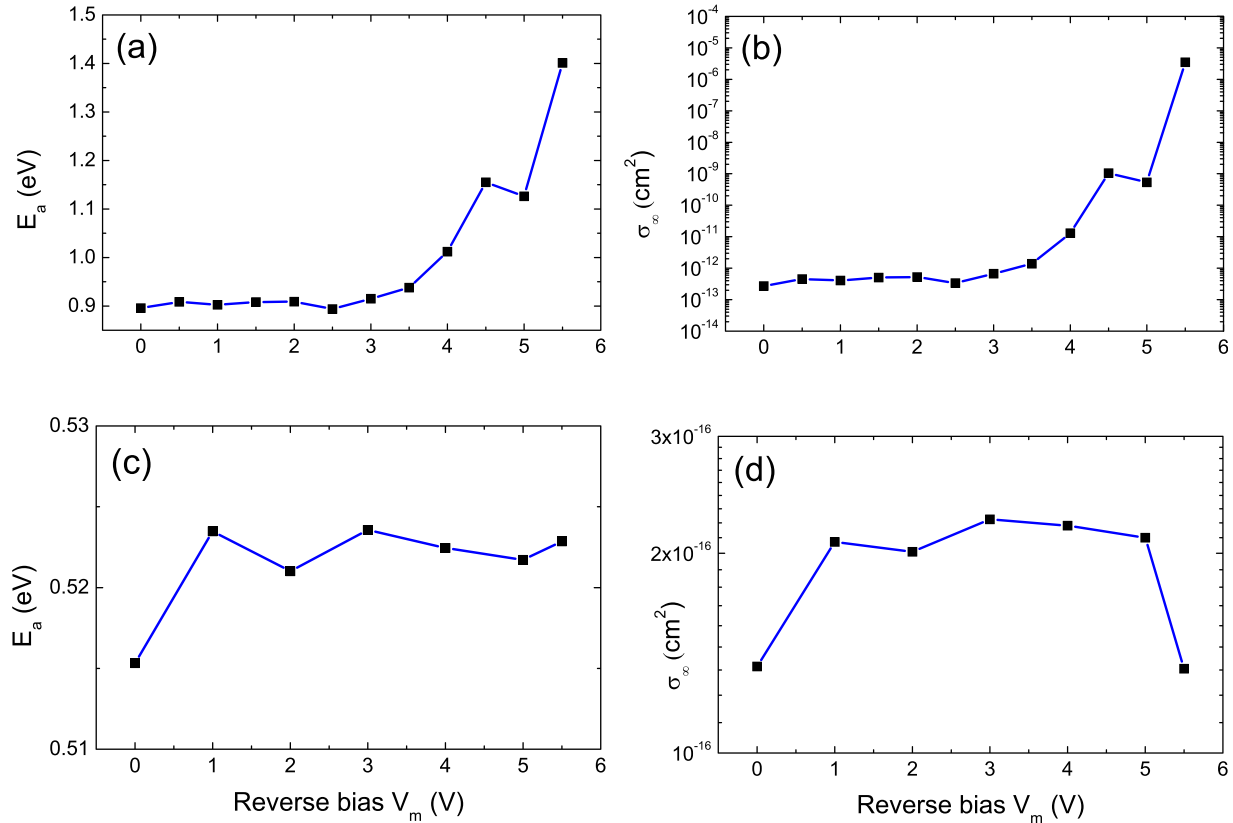


FIG. 3. Activation energies and apparent capture cross-sections extracted from the charge selective DLTS measurements. Sample C (QDs + AIP barrier): (a) E_a , (b) σ_∞ ; Sample B (AIP barrier only): (c) E_a , (d) σ_∞ .

each other. On closer inspection, their activation energies and capture cross-sections are compatible within their experimental error ($E_a = 1.12(\pm 0.04)$ eV, $\sigma_\infty = 5(\pm 5) \times 10^{-10}$ cm² and $E_a = 1.16(\pm 0.02)$ eV, $\sigma_\infty = 1.1(\pm 0.5) \times 10^{-9}$ cm², respectively) and we therefore interpret the two data points as originating from the same internal level in the QDs. We thus decide to discard the data relative to the point at $V_m = 5.5$ V as an artefact and assign to the QDs + AIP system a localization energy of $1.14(\pm 0.04)$ eV with an associated capture cross-section of $7(\pm 5) \times 10^{-10}$ cm² (from evaluation of the data relative to the points at $V_m = 5.0$ V and $V_m = 4.5$ V, grouped together). We attribute the 0.90 ± 0.01 eV localization visible for $V_r \leq 2.5$ V to the effect of the barrier.

The number of holes per QD involved in each charge-selective DLTS measurement can be extracted directly from the maximum amplitude of the DLTS signal. Since we are observing the charging and discharging of a single internal level of the QDs, we expect 2 holes per QD to be involved in the process. Assuming a density of QDs of 1×10^{10} cm⁻², which is an order of magnitude lower than previously reported,¹¹ we do indeed obtain a value of about 2 for each reverse bias point (average: 2.1 ± 0.3 holes/QD).

A similar charge-selective DLTS measurement was carried out also on sample B. The value of the activation energy oscillates around $0.52(\pm 0.05)$ eV for all voltages (see Fig. 3(c)), with an average capture cross-section of $2.1(\pm 0.6) \times 10^{-16}$ cm² (Fig. 3(d)). This localization effect is interpreted as caused by the barrier, for which we expect a height of about 0.50 eV.²⁰ This value is 0.38 eV short of the 0.90 eV seen in sample C at low voltages. The reason is that

the value of 0.90 eV does not represent the height of the AIP barrier alone, but rather the combined effect of the barrier and the QDs. The highest bound level in the QDs is deeper into the bandgap than the top of the valence band and therefore contributes additional localization energy (see Fig. 2 for a sketch of the emission process).

We can estimate the storage time at room temperature using Eq. (1). The value for Sample C, which amounts to $230(\pm 60)$ s, is plotted in Fig. 4 together with values already available in literature.^{5,6,9,21,22} The large error associated with the estimate (26%) is due to the low accuracy in the estimate of the capture cross-section, which is an intrinsic

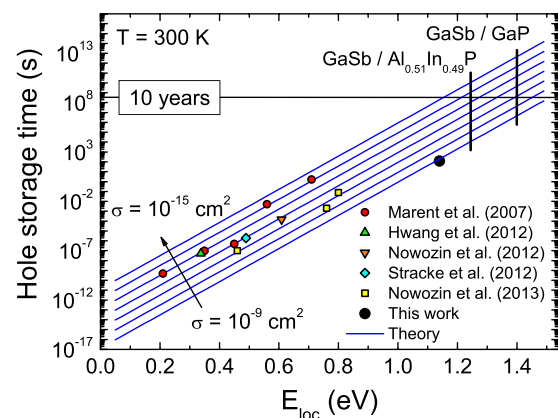


FIG. 4. Hole storage time in QDs vs localization energy. Lines represent the theoretical relationship for capture cross sections ranging from 10^{-9} to 10^{-15} cm². Values from Refs. 6, 9, 21, 22, and 5. A review of all measured and predicted values can be found in Ref. 23.

problem of evaluation using the Arrhenius plot. Nonetheless, even within the error margin the storage time of Sample C represents an improvement of 2 orders of magnitude compared to the previous record of 1.6 s for GaSb QDs in GaAs with an $\text{Al}_{0.9}\text{Ga}_{0.1}\text{As}$ barrier.⁶ It is interesting to note that a localization energy in the order of the one demonstrated in this work (1.14 eV) would already suffice for non volatility (i.e., storage time > 10 yr), provided that the capture cross section was $\leq 4 \times 10^{-14} \text{cm}^2$. The most viable way to achieve longer storage times is by further increasing the localization energy using different material combinations. Good candidate materials are, for example, GaSb/ $\text{Al}_{0.51}\text{In}_{0.49}\text{P}$ QDs (estimate: $E_{loc} = 1.25 \text{eV}$) and GaSb/GaP QDs (estimate: $E_{loc} = 1.4 \text{eV}$).^{20,24}

Another way of increasing the storage time would be engineering of the capture cross-section. This parameter depends on several factors, including hole wave functions in the QDs, coupling to phonons, and Auger scattering. An effective method of modelling these effects with relation to the capture cross section has yet to be developed. A way to shrink the capture cross-section could be to reduce the size of the QDs. This can be accomplished by reducing the length of the growth interruption after QD deposition during epitaxial growth,¹¹ but at the expense of a reduced localization energy of charge carriers in the QDs. Further investigation is needed before successfully employing this method for capture cross-section engineering.

In summary, we studied the electrical properties of 3 GaP samples consisting of an n^+p -diode containing a sole AIP barrier or $\text{In}_{0.5}\text{Ga}_{0.5}\text{As}$ QDs with an AIP barrier, alongside a reference sample. We used DLTS to determine the activation energies for the latter two structures, which are $0.52(\pm 0.05) \text{eV}$ and $1.14(\pm 0.04) \text{eV}$, respectively. Subtracting the former figure from the latter yields an estimate for the localization energy of simple $\text{In}_{0.5}\text{Ga}_{0.5}\text{As}$ QDs in GaP of $0.62(\pm 0.06) \text{eV}$. This value is in good agreement with the theoretically expected 0.6eV .⁷ Moreover, the increase from the 0.49eV we measured previously for $\text{In}_{0.25}\text{Ga}_{0.75}\text{As}$ QDs in GaP⁹ is compatible with the fact that the previous measurement was a *mean* activation energy and that the In content has been increased from 25% to 50%.⁷ We demonstrated a hole storage time at room temperature of $230(\pm 60) \text{s}$ for the sample containing QDs and an AIP barrier. In order to further increase the localization energy and the storage time, we propose keeping GaP as the matrix material and advancing the material system to GaSb/(Ga,Al)P QDs.

The authors acknowledge the support by the DFG Contract No. BI284/29-1 and BMBF Project HOFUS 16V0196. The project's work of some of the authors was

funded by the Deanship of Scientific Research (DSR), King Abdulaziz University, under Grant No. 2-4-1432/HiCi. These authors, therefore, acknowledge DSR technical and financial support.

¹“International technology roadmap for semiconductors,” 2009, PDF available at http://www.itrs.net/Links/2009ITRS/2009Chapters_2009Tables/2009_ERD.pdf.

²A. Marent, T. Nowozin, M. Geller, and D. Bimberg, *Semicond. Sci. Technol.* **26**, 014026 (2011).

³M. Geller, A. Marent, T. Nowozin, D. Bimberg, N. Akçay, and N. Öncan, *Appl. Phys. Lett.* **92**, 092108 (2008).

⁴A. Marent, T. Nowozin, J. Gelze, F. Luckert, and D. Bimberg, *Appl. Phys. Lett.* **95**, 242114 (2009).

⁵T. Nowozin, L. Bonato, A. Högner, A. Wiengarten, D. Bimberg, W.-H. Lin, S.-Y. Lin, C. J. Reyner, B. L. Liang, and D. L. Huffaker, *Appl. Phys. Lett.* **102**, 052115 (2013).

⁶A. Marent, M. Geller, A. Schliwa, D. Feise, K. Pötschke, D. Bimberg, N. Akçay, and N. Öncan, *Appl. Phys. Lett.* **91**, 242109 (2007).

⁷C. Robert, C. Cornet, P. Turban, T. Nguyen Thanh, M. O. Nestokoln, J. Even, J. M. Jancu, M. Perrin, H. Folliot, T. Rohel, S. Tricot, A. Balocchi, D. Lagarde, X. Marie, N. Bertru, O. Durand, and A. Le Corre, *Phys. Rev. B* **86**, 205316 (2012).

⁸Vurgaftman and Meyer²⁰ report for the measured valence-band discontinuity in GaP/AIP heterostructures values in the $0.34\text{--}0.69 \text{eV}$ range and recommend using $\Delta E_v = 0.47 \text{eV}$.

⁹G. Stracke, A. Glacki, T. Nowozin, L. Bonato, S. Rodt, C. Prohl, A. Lenz, H. Eisele, A. Schliwa, A. Strittmatter, U. W. Pohl, and D. Bimberg, *Appl. Phys. Lett.* **101**, 223110 (2012).

¹⁰C. Prohl, A. Lenz, D. Roy, J. Schuppang, G. Stracke, A. Strittmatter, U. W. Pohl, D. Bimberg, H. Eisele, and M. Dähne, *Appl. Phys. Lett.* **102**, 123102 (2013).

¹¹G. Stracke, E. M. Sala, S. Selve, T. Niermann, A. Schliwa, A. Strittmatter, and D. Bimberg, *Appl. Phys. Lett.* **104**, 123107 (2014).

¹²D. V. Lang, *J. Appl. Phys.* **45**, 3023 (1974).

¹³T. Nowozin, A. Marent, M. Geller, D. Bimberg, N. Akçay, and N. Öncan, *Appl. Phys. Lett.* **94**, 042108 (2009).

¹⁴The hole emission processes from the QDs used here were not again investigated. The structure we used is very similar to the one used by Nowozin *et al.*,¹³ such that their results apply also in the present case.

¹⁵P. Blood and J. W. Orton, *The Electrical Characterization of Semiconductors: Majority Carriers and Electron States* (Academic, London, 1992).

¹⁶V. Rideout, *Solid State Electron.* **18**, 541 (1975).

¹⁷I. Mojzes, T. Sebestyén, and D. Szigethy, *Solid State Electron.* **25**, 449 (1982).

¹⁸V. Malina and R. Soukupová, *Thin Solid Films* **125**, L21 (1985).

¹⁹M. Geller, C. Kapteyn, L. Müller-Kirsch, R. Heitz, and D. Bimberg, *Appl. Phys. Lett.* **82**, 2706 (2003).

²⁰I. Vurgaftman and J. R. Meyer, *J. Appl. Phys.* **89**, 5815 (2001).

²¹J. Hwang, A. J. Martin, J. M. Millunchick, and J. D. Phillips, *J. Appl. Phys.* **111**, 074514 (2012).

²²T. Nowozin, A. Marent, L. Bonato, A. Schliwa, D. Bimberg, E. P. Smakman, J. K. Garleff, P. M. Koenraad, R. J. Young, and M. Hayne, *Phys. Rev. B* **86**, 035305 (2012).

²³T. Nowozin, D. Bimberg, K. Daqrouq, M. N. Ajour, and M. Awedh, *J. Nanomater.* **2013**, 215613.

²⁴D. Bimberg, A. Marent, T. Nowozin, and A. Schliwa, *Proc. SPIE* **7947**, 79470L (2011).